

EXPERIMENTAL INVESTIGATION OF THE LIQUID VOLUMETRIC MASS TRANSFER COEFFICIENT FOR UPWARD GAS-LIQUID TWO-PHASE FLOW IN RECTANGULAR MICROCHANNELS

X. Y. Ji, Y. G. Ma^{*}, T. T. Fu, CH. Y. Zhu and D. J. Wang

School of Chemical Engineering and Technology, State Key Laboratory of Chemical Engineering,
Tianjin University, Tianjin 300072, China.
E-mail: ygma@tju.edu.cn

(Submitted: June 30, 2010 ; Revised: August 2, 2010 ; Accepted: August 26, 2010)

Abstract - The gas-liquid two-phase mass transfer process in microchannels is complicated due to the special dynamical characteristics. In this work, a novel method was explored to measure the liquid side volumetric mass transfer coefficient $k_{L,a}$. Pressure transducers were utilized to measure the pressure variation of upward gas-liquid two-phase flow in three vertical rectangular microchannels and the liquid side volumetric mass transfer coefficient $k_{L,a}$ was calculated through the Pressure-Volume-Temperature correlation of the gas phase. Carbon dioxide-water, carbon dioxide-ethanol and carbon dioxide-n-propanol were used as working fluids, respectively. The dimensions of the microchannels were $40\ \mu\text{m}\times 240\ \mu\text{m}$ (depth \times width), $100\ \mu\text{m}\times 800\ \mu\text{m}$ and $100\ \mu\text{m}\times 2000\ \mu\text{m}$, respectively. Results showed that the channel diameter and the capillary number influence $k_{L,a}$ remarkably and that the maximum value of $k_{L,a}$ occurs in the annular flow regime. A new correlation of $k_{L,a}$ was proposed based on the Sherwood number, Schmidt number and the capillary number. The predicted values of $k_{L,a}$ agreed well with the experimental data.

Keywords: Microchannels; Gas-liquid upward two-phase flow; Mass transfer; Pressure variation.

INTRODUCTION

The gas-liquid two-phase micro-contactors are a very important part of micro-chemical systems. The interfacial area - to - volume ratio of gas-liquid two-phase flow in microchannels was demonstrated to be much higher than that in conventional tubes (Haverkamp et al., 2001; Yue et al., 2006; Fu et al., 2010) and the mass transfer process was greatly enhanced. Therefore, microchannels could be used efficiently and safely in gas absorption, desorption, direct fluorination, hydrogenation and other processes (Tegrotenhuis et al., 2000; Jähnisch et al., 2000; Demas et al., 2003; Yeong et al., 2004;

Kobayashi et al., 2004). There are many reports (Jepsen, 1970; Irandoust and Andersson, 1988; Irandoust et al., 1992; Tortopidis and Bontozoglou, 1997; Bercic and Pintar, 1997; Kreutzer, 2003; Van Baten and Krishna, 2004; Vandu et al., 2005; Yue et al., 2009) on the gas-liquid two-phase mass transfer process. Because of the significant effect of surface tension on gas-liquid two-phase flow in microchannels, the characteristics of gas-liquid two-phase flow in microchannels are quite different from those in conventional channels. Consequently, a fundamental understanding of the gas-liquid mass transfer process in microchannels is very necessary.

*To whom correspondence should be addressed

Although titration methods show good accuracy in determining the concentration of solute in solutions, their disadvantage is also obvious. For instance, a large amount of solution is required and the determination of the endpoint often depends on artificial factors. In microchannels 100 μm in magnitude, the titration method is quite limited by the small volumetric flow rates of gas and liquid phases. Moreover, trace absorption and real-time observation and measurement are very difficult. In this paper, a high-speed camera and pressure transducers were utilized, respectively, to directly observe the flow pattern and measure the pressure change for upward gas-liquid two-phase flow in real-time in three vertical rectangular microchannels. The liquid volumetric mass transfer coefficient $k_{L,a}$ was calculated based on the Pressure-Volume-Temperature correlation of the gas phase. The experimental results at high flow rates were verified by the titration method and the capillary number Ca was introduced to correlate the liquid volumetric mass transfer coefficient $k_{L,a}$.

EXPERIMENTAL SETUP

The microchannel chips were fabricated first by the etching technique on transparent glass and then the mechanical method was applied to produce and polish the microchannels with rectangular cross-section. Dimensions of the microchannels were 40 μm \times 240 μm (depth \times width), 100 μm \times 800 μm and 100 μm \times 2000 μm , respectively, referred to as microchannels 1, 2 and 3 for short. The length of the two-phase inlets and mixing section were 1.5 and 4cm, respectively, as shown in Figure 1 (a). The hydraulic diameters d_h of the microchannels were 68.57 μm , 177.78 μm and 190.48 μm , respectively, and all the experiments were carried out at atmospheric pressure and 298.15K.

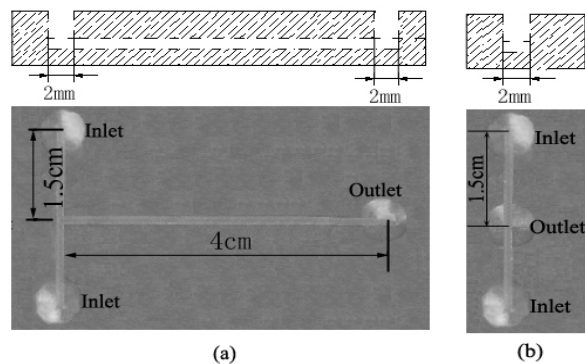


Figure 1: The rectangular microchannel chip. (a) with two-phase mixing section; (b) without two-phase mixing section

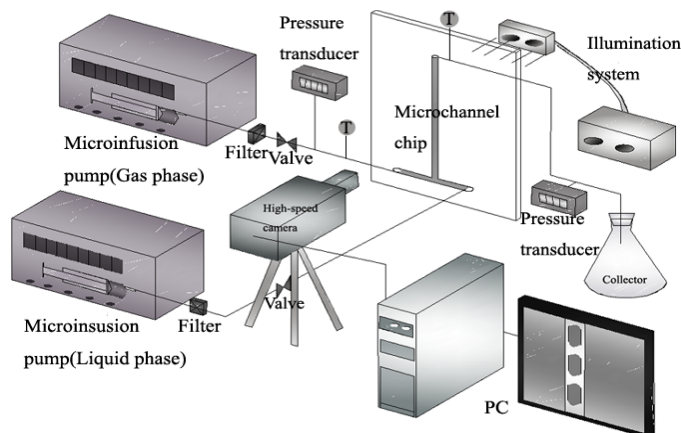
To eliminate the effect of outlet connecting tubes and two-phase collectors on the mass transfer of two-phase mixing sections, absorption in non-mixing section microchannels was conducted under the same conditions (named blank experiments), but, as shown in Figure 1(b), the T-junction was connected directly to the outlet connecting tubes without the mixing section.

The flow chart of experiments is shown in Figure 2. Pure carbon dioxide was driven and the flow rates were set by a micro-infusion pump. After flowing through a filter and a valve, it was then injected into the vertical microchannels. The pressure transducer installed on the gas inlet connecting pipe determines the inlet pressure of the microchannels. Water was boiled to remove the dissolved carbon dioxide and then cooled to room temperature. Water, ethanol and n-propanol (physical properties are listed in Table 1) were driven by the micro-infusion pump and the actual flow rates of the liquid phases were determined by using an electronic balance. Liquid phase and carbon dioxide flowed in the mixing section of microchannels and then into the two-phase collector through an outlet connecting tube of 0.5mm diameter. The two-phase collector was enclosed to isolate it from the outside environment. The pressure transducer installed on the outlet connecting tube measured the outlet pressure of the microchannels and two thermocouple thermometers installed on the inlet and outlet connecting tubes were employed to determine the temperature of the system. A high-speed camera (2500fps) was used for the observation of the flow patterns. The mass transfer of carbon dioxide into the liquid phases was determined by the Pressure-Volume-Temperature correlation of the gas phase based on the pressure variation before and after the absorption. The titration method was used to verify the pressure method at large flow rates. For this purpose, 10mL of 0.1mol·L⁻¹ NaOH solution were added to 10mL of the two-phase mixture and then 0.1mol·L⁻¹ HCl solution was used for titration; phenolphthalein and helianthine were used as the first and second endpoint indicators (light pink and orange), respectively. The results showed that the relative deviation of the two methods at large flow rates was 1~2.5%, which confirmed the credibility of the pressure variation method.

To eliminate the effect of the frictional pressure drop on the experimental results, the frictional pressure drop of nitrogen-water, without absorption, was measured experimentally. The frictional pressure drop for nitrogen-ethanol and nitrogen-n-propanol without absorption were calculated based on the model of Lockhart and Martinelli (1949) and the method of Chisholm (1967).

Table 1: Physical properties of the various liquid systems used

Liquid phase	Viscosity μ , Pa·s	Surface tension σ , N·m ⁻¹	μ/σ , s·m ⁻¹
Water	1.005×10^{-3}	72.8×10^{-3}	0.0138
Ethanol	1.2×10^{-3}	22.27×10^{-3}	0.0539
N-propanol	2.256×10^{-3}	23.71×10^{-3}	0.0952

**Figure 2: The flow chart of the experiment**

The Lockhart and Martinelli model could be expressed via Eqs. (1) and (2):

$$(\Delta P_F/L)_t = \phi_L^2 \times (\Delta P_F/L)_L \quad (1)$$

$$X^2 = (\Delta P_F/L)_L / (\Delta P_F/L)_g \quad (2)$$

where $(\Delta P_F/L)_t$ is the total two-phase frictional pressure drop in the microchannels, kPa·m⁻¹; $(\Delta P_F/L)_L$ is the liquid single-phase frictional pressure drop in the microchannels, kPa·m⁻¹; $(\Delta P_F/L)_g$ is the gas single-phase frictional pressure drop in the microchannels, kPa·m⁻¹. ϕ_L^2 is the two-phase multiplier and X is the Martinelli parameter.

Chisholm related ϕ_L^2 to X by introducing another parameter, the Chisholm factor C :

$$\phi_L^2 = 1 + (C/X) + (1/X^2) \quad (3)$$

A new correlation of the Chisholm factor C that takes into account the different physical properties of the liquid phases was proposed in our previous work and was employed to calculate the frictional pressure drop of nitrogen-ethanol and nitrogen-n-propanol without absorption. The correlation expressed as follows:

$$C = aCa_L^b \quad (4)$$

where $Ca_L = \mu_L J_L / \sigma$,

$$a = 7.59 - 0.4237 \times A^{-0.9485} + 0.0023 \times Re_L$$

and $b = 0.223 + 0.2 \times A^{0.9778}$. A is the aspect ratio of the rectangular cross-section of the microchannels. Thus, the practical pressure change resulting from absorption could be derived by subtracting the frictional pressure drop from the total pressure change.

RESULTS AND DISCUSSION

Flow Patterns of Upward Two-Phase Flow in Vertical Microchannels

The gas-liquid two-phase flow patterns captured by the high-speed camera in the experiments are shown in Figure 3. The flow patterns varied from Taylor bubble flow to annular flow with increasing gas and liquid flow rates. The length of the gas bubbles L_B and liquid slugs L_S in Taylor bubble flow were obtained from an analysis of flow pattern images. Figure 4 shows the experimental results for Taylor bubble length and slug length. As can be seen from Figure 4, the distribution of the length of Taylor bubbles and liquid slugs became gradually uniform from water to ethanol and to n-propanol as the continuous phase, which indicated that there was a better mixing effect and mass transfer performance in the carbon dioxide-n-propanol system than in the other two systems.

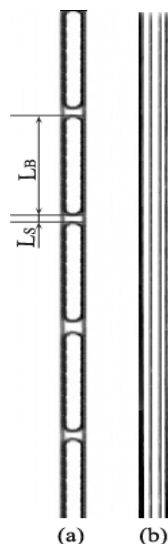


Figure 3: Flow patterns of upward two-phase flow in the microchannels (a) Taylor bubble flow; (b) Annular flow

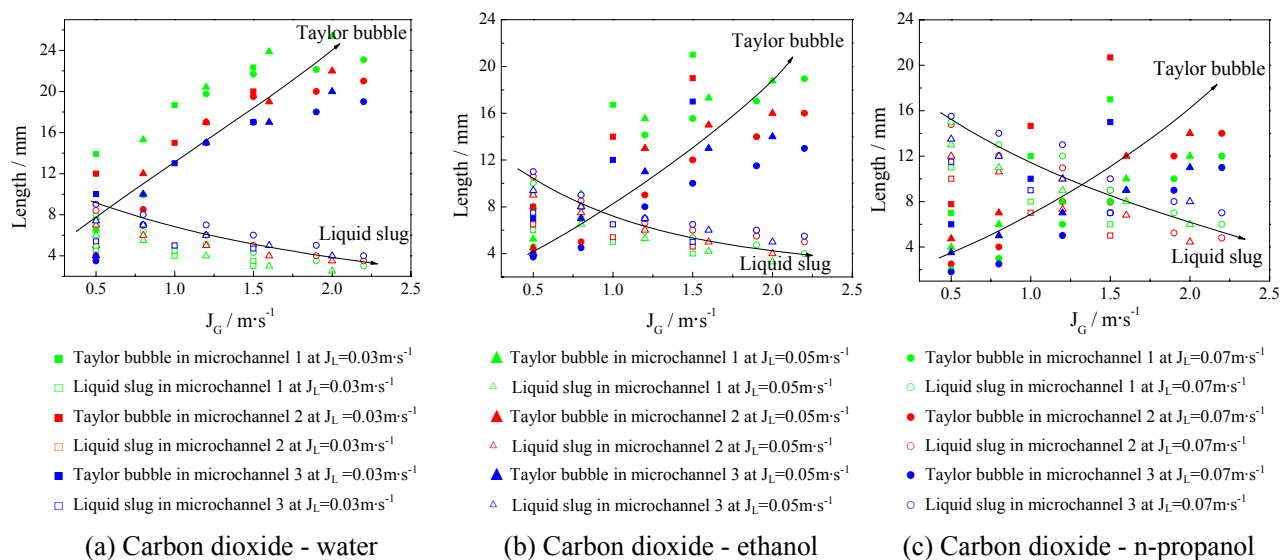


Figure 4: The Taylor bubble lengths and liquid slug lengths in microchannels 1, 2 and 3 (a) Carbon dioxide – water; (b) Carbon dioxide – ethanol; (c) Carbon dioxide – n-propanol

Calculation of the Liquid Volumetric Mass Transfer Coefficient $k_{L,a}$

The mass transfer of carbon dioxide into water, ethanol and n-propanol is mainly governed by the liquid phase and $k_{L,a}$ is obtained from the equation of mass balance (Yue et al. (2006)):

$$k_{L,a} = \frac{J_L}{L_C} \ln\left(\frac{c_e - c_0}{c_e - c_1}\right) \quad (5)$$

where C_0 and C_1 are concentrations of carbon dioxide in the liquid phase at the inlet and outlet of the microchannels and C_e is the equilibrium concentration of carbon dioxide in the liquid phase (Zhang, 1986; Liu et al., 2002), J_L is the liquid phase superficial velocity and L_C is the length of the mixing section of the microchannel. The value of $k_{L,a}$ in the outlet connecting tube of the experiments is the same as that of the blank experiments, expressed as follow:

$$\ln\left(\frac{c_e - c_1}{c_e - c_2}\right) = \ln\left(\frac{c_e - c_2'}{c_e - c_2}\right) \quad (6)$$

Yue et al. (2006) demonstrated that Eq. (6) could reasonably eliminate the outlet effect. Combination of Eq. (5) and Eq. (6) results in the following expression:

$$k_{L,a} = \frac{J_L}{L_C} \ln\left(\frac{c_e - c_2'}{c_e - c_2}\right) \quad (7)$$

where C_2 and C_2' are the concentrations of carbon dioxide in the liquid phases in the two-phase collector of the microchannel flow experiments and the blank experiments, respectively, and are calculated from the following correlations:

$$C_2 = \frac{V_{CO_2} P_{in} - V(P_{oa} - P_{ob})}{RTV_{liquid}} \quad (8)$$

$$C_2' = \frac{V_{CO_2}' P_{in}' - V(P_{oa}' - P_{ob}')}{RT'V_{liquid}'} \quad (9)$$

where P_{in} is the inlet pressure of the absorption processes and P_{in}' is that of the blank experiments; P_{ob} is the outlet pressure before absorption in the experiments and P_{ob}' is that of the blank experiments; P_{oa} is the outlet pressure after absorption in the experiments and P_{oa}' is that of the blank experiments; T is the temperature of system in the experiments and T' is that of the blank

experiments; V_{CO_2} is the total CO_2 volume injected into the system in the experiments and V_{CO_2}' is that of the blank experiments; V_{liquid} is the total liquid phase volume injected into the system in the experiments and V_{liquid}' is that of the blank experiments; and V is the total volume of the system.

A large amount of experimental data has been measured for calculating $k_{L,a}$. Table 2 lists typical measured values for the quantities on the r.h.s. of Eqs. (8) and (9) of the three systems in microchannel 1 at $J_L=0.05m\cdot s^{-1}$ and $J_G=1.8 m\cdot s^{-1}$.

Liquid Volumetric Mass Transfer Coefficient $k_{L,a}$

Figure 5 and Figure 6 illustrate the influences of channel diameter and capillary number on $k_{L,a}$, respectively, with the liquid phase superficial velocities $J_L=0.03, 0.05$ and $0.07 m\cdot s^{-1}$ from bottom to top, respectively; the transition from Taylor bubble flow to an annular flow pattern is marked by black lines.

It can be seen from Figures 5 and 6 that the value of $k_{L,a}$ in microchannel 1 was much larger than that in microchannels 2 and 3. The values of $k_{L,a}$ also presented remarkable differences between the different liquid phases used, which demonstrated the great influence of both channel diameter and liquid phase capillary number on $k_{L,a}$. The value of $k_{L,a}$ increased with gas and liquid superficial velocities, because, in Taylor bubble flow, the number of gas bubbles increased with increasing the gas flow rate. As a consequence, the interfacial area for mass transfer was enhanced, resulting in the increase of $k_{L,a}$. The value of $k_{L,a}$ achieved the maximum in the annular flow, in accord with the literature (Haverkamp et al., 2001; Kobayashi et al., 2004).

Table 2: The typical values of pressure and volume on the r.h.s. of Eqs. (8) and (9) for the three systems in microchannel 1.

system pressure and volume	Carbon dioxide-water	Carbon dioxide-ethanol	Carbon dioxide-n-propanol
P_{in}	126.925	129.025	131.425
P_{in}'	122.525	123.825	126.225
P_{ob}	101.725	101.925	102.125
P_{ob}'	101.725	101.825	101.925
P_{oa}	102.225	102.325	102.425
P_{oa}'	101.925	102.025	102.125
V_{CO_2}	6×10^{-6}	6×10^{-6}	6×10^{-6}
V_{CO_2}'	6×10^{-6}	6×10^{-6}	6×10^{-6}
V_{liquid}	0.12×10^{-6}	0.12×10^{-6}	0.12×10^{-6}
V_{liquid}'	0.12×10^{-6}	0.12×10^{-6}	0.12×10^{-6}
V	0.1×10^{-6}	0.1×10^{-6}	0.1×10^{-6}

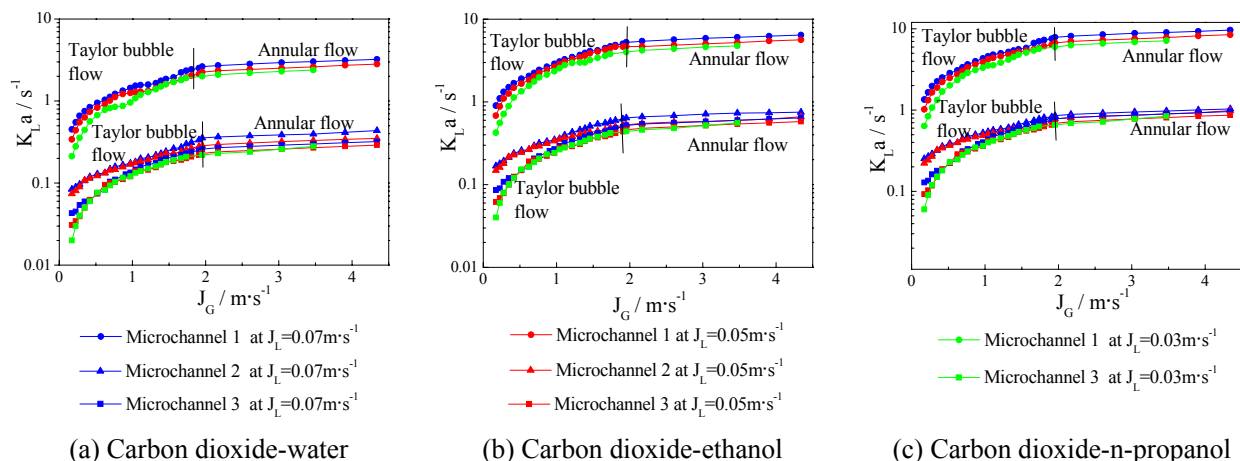


Figure 5: Influence of the channel diameter on $k_L a$ (a) Carbon dioxide – water; (b) Carbon dioxide – ethanol; (c) Carbon dioxide – n-propanol

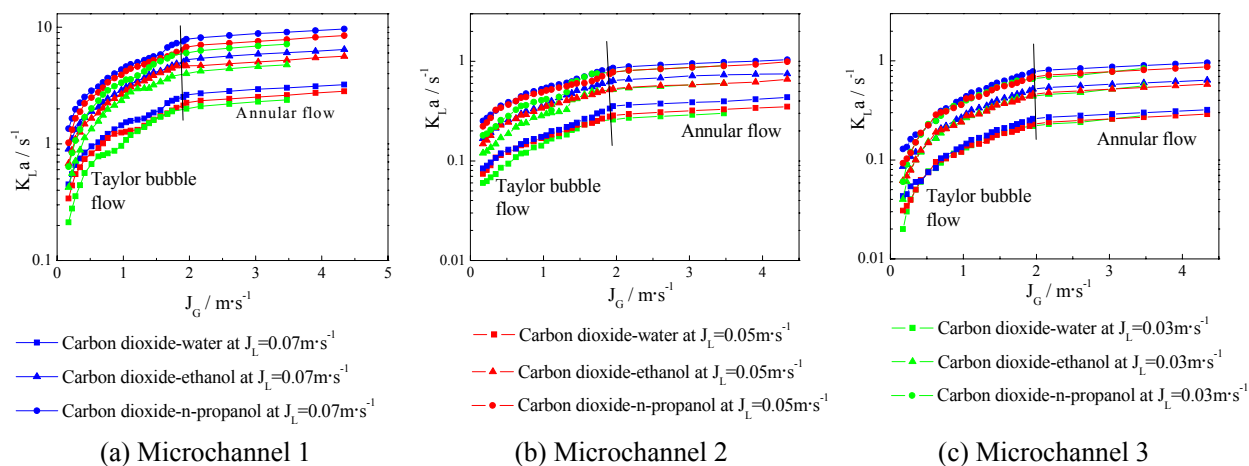


Figure 6: Influence of the capillary number on $k_L a$ (a) Microchannel 1; (b) microchannel 2; (c) Microchannel 3

There are many reports on the investigation of the liquid mass transfer coefficient $k_L a$ in Taylor bubble flow. Jepsen (1970) proposed an energy dissipation model to correlate the value of $k_L a$ and the pressure drop of the system is required to use this model. Bercic and Pintar (1997) studied the absorption of methane into water in a circular tube and proposed a model of $k_L a$ that did not consider the influence of tube diameter and diffusion coefficient. Subsequently, researchers divided the mass transfer of the Taylor bubble to the surrounding liquid into three parts, the cap and tail of bubbles into the liquid slug, and the cylindrical part of bubble into the liquid film between the gas bubble and the tube wall. On the basis of this, Van Baten and Krishna (2004) simulated the mass transfer process of a Taylor bubble rising into the surrounding liquid in vertical

circular tubes with CFD and proposed a model of $k_L a$ that introduced the tube diameter and diffusion coefficient, as follows:

$$k_L a = \frac{2}{\sqrt{\pi}} \sqrt{\frac{D J_B}{(L_B - d_h) d_h (L_B + L_S)}} \frac{4(L_B - d_h)}{d_h (L_B + L_S)} + 2 \frac{\sqrt{2}}{\pi} \sqrt{\frac{D J_B}{d_h}} \frac{4}{(L_B + L_S)} \quad (10)$$

where J_B is the rising velocity of the Taylor bubble, approximately given by $J_B \approx J_L + J_G$, as validated by analyzing the variation of flow pattern images, D is the liquid phase diffusivity, and the Taylor bubble length and liquid slug length were obtained by visualization and measurement of flow pattern

images captured with a high speed camera. Van Baten and Krishna (2004) regarded the mass transfer of the cylindrical part of the bubble into the liquid film as the dominant part of the total mass transfer process. Based on this, Vandu et al. (2005) investigated the mass transfer process of oxygen into water in circular and square channels of 1mm, 2mm and 3mm diameters and proposed a model of $k_L a$ that approximated the total mass transfer as being only that of the cylindrical part transferring into the film. Yue et al. (2009) also investigated the absorption of oxygen into water experimentally in an air-water system and proposed a correlation of $k_L a$ according to Eq. (10).

The precise length of the Taylor bubbles and liquid slugs is required to apply the above models, which results in great limitations in application. Yue et al. (2006) utilized the Sherwood number and Schmidt number to correlate $k_L a$ in a rectangular microchannel with a hydraulic diameter of $667\mu\text{m}$, as follows:

$$\frac{Sh_L ad_h}{Sc_L^{0.5}} = 0.0439 Re_G^{0.394} Re_L^{0.905} \quad (11)$$

where the Sherwood number is $Sh_L = k_L d_h / D$, the Schmidt number $Sc_L = \mu_L / \rho_L D$, the gas phase Reynolds number $Re_G = \rho_G J_G d_h / \mu_G$ and liquid phase Reynolds number $Re_L = \rho_L J_L d_h / \mu_L$, with μ_L, μ_G and ρ_L, ρ_G as the viscosities and densities of the liquid and gas phases, respectively.

Figure 7 shows the comparison of experimental results for carbon dioxide-water with values predicted by Eqs. (10) and (11). Because the results of carbon dioxide-ethanol and carbon dioxide-n-propanol showed the same trends as that of carbon dioxide-water, they are not displayed here. It can be seen from Figure 6 that there exists a remarkable deviation between the experimental results and values predicted by Eqs. (10) and (11). This may be explained as follows: Eq. (10) considers that the mass transfer of the cylindrical part into the liquid film dominates the total mass transfer; the mass transfer into the liquid film is thus mainly controlled by the length of the liquid slugs surrounding the Taylor bubbles. The longer the liquid slugs, the easier the absorbed gas phase is transferred into the liquid slugs from the liquid film. As a consequence, the liquid film could absorb more gas phase, which results in the high value of $k_L a$ (Van Baten and Krishna, 2004; Vandu et al., 2005; Yue et al., 2009). However, the hydraulic diameters of the

microchannels used in our experiments were $100\mu\text{m}$ in magnitude, such that the lengths of the liquid slugs were much shorter than those ($L_S > 3L_B$) in large tubes. Consequently, the gas phase absorbed by the liquid film could not be transferred into the liquid slugs efficiently. Therefore, the liquid film achieved saturation and could not absorb any more gas phase; in this case, the experimental results for $k_L a$ were much lower than those of the literature. The predictive performance of Eq. (11) is better than that of Eq. (10) and appears to be quite well consistent with experimental results in the range of $Re_L = 59.4 \sim 700.6$ and $Re_G = 62.1 \sim 1088.3$. However, it is worth noting that the ranges of gas and liquid Reynolds numbers in the present experiments were $Re_L = 1.1 \sim 13.07$ and $Re_G = 0.87 \sim 61.9$, respectively. The hydraulic diameters of microchannels were also much smaller than the $667\mu\text{m}$ used by Yue et al. (2006), resulting in the large deviation of more than 20% of the predictions of by Eq. (11) from the experimental data in this work, as shown in Fig.6.

The hydraulic diameters of the microchannels used here were all less than $200\mu\text{m}$. On such a micro-scale, the capillary number Ca has an important influence on gas-liquid two-phase flow, which was demonstrated by the remarkable difference of the experimental results between water, ethanol and n-propanol as the working liquid phase. Thus, in this paper, a new correlation is proposed based on Eq. (11) but introducing the liquid phase capillary number Ca_L :

$$\frac{Sh_L ad_h}{Sc_L} = 0.22 Ca_L^{0.7586} Re_G^{0.78} Re_L^{0.0535} \quad (12)$$

where $Ca_L = \mu_L J_L / \sigma$, with σ being the surface tension. The values of the parameters were obtained by using the least square fitting method. The comparison between experimental results and values predicted by Eq. (12) is shown in Figure 8. The mean deviations are 10.5%, 13.75% and 15.06% for carbon dioxide-water, 11.65%, 8.05% and 6.93% for carbon dioxide-ethanol and 12.16%, 10.27% and 12.13% for carbon dioxide-n-propanol in the three microchannels, respectively. Figure 9 shows the comparison of predictions of Eq. (12) with experimental data in the circular channels of Van Baten and Krishna (2004) and in the rectangular channel of Yue et al. (2006); the mean deviations are 4.82% and 4.19%, respectively, indicating that Eq. (12) has good predictive performance in both circular and rectangular microchannels.

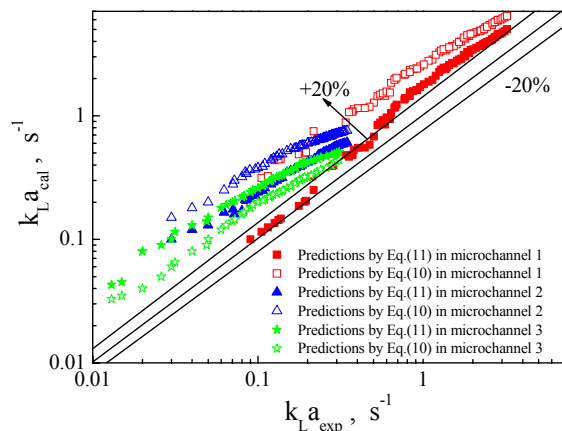


Figure 7: Comparison of results predicted by Eq. (10) and (11) with the present experimental data

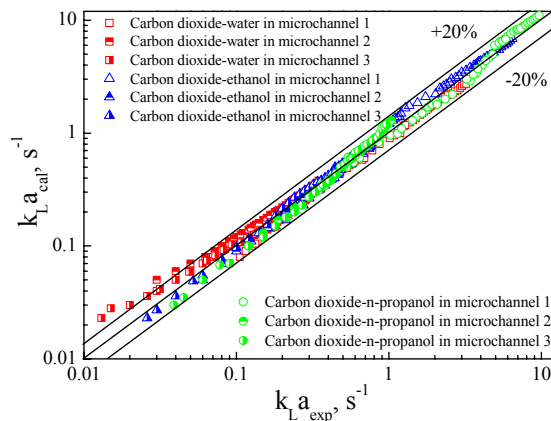


Figure 8: Comparison of predictions of Eq. (12) and experimental results in this work

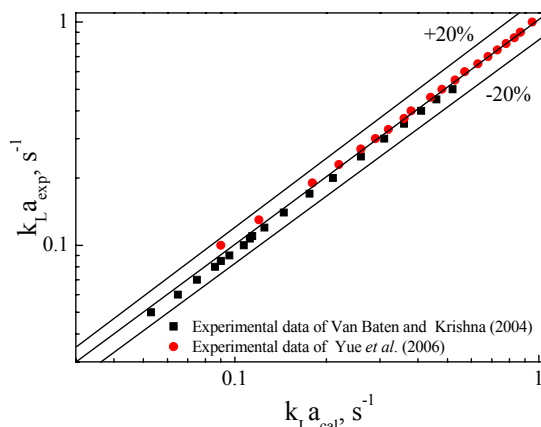


Figure 9: Comparisons of experimental data of Van Baten and Krishna (2004) and Yue et al. (2006) and predictions of Eq. (12)

CONCLUSIONS

The liquid volumetric mass transfer coefficient $k_L a$ of carbon dioxide-water, carbon dioxide-ethanol and carbon dioxide-n-propanol two-phase upward flow in vertical microchannels were obtained by measuring the pressure variation before and after the absorption processes. The experimental results were checked by titration under large flow rates and the following conclusions could be obtained:

1) Determination of the liquid volumetric mass transfer coefficient $k_L a$ via measuring the pressure variation of the system before and after the absorption process has the advantage of a non-interfering, real-time determination, high credibility, and good accuracy for trace absorption and requires very little solution, being suitable for the micro-scale;

2) Both the channel diameter and the liquid phase capillary number influence the liquid volumetric

mass transfer coefficient remarkably, and $k_L a$ achieves its maximum in the annular flow pattern;

3) A new dimensionless correlation of $k_L a$ was proposed by introducing the liquid phase capillary number, which showed good predictive performance under micro-scale conditions.

ACKNOWLEDGEMENTS

This work was supported by the National Nature Science Foundation of China (No. 20876107) and the Opening Project of State Key Laboratory of Chemical Engineering (No. SKL-ChE-08B06).

NOMENCLATURE

a Ratio of interfacial area to volume $\text{m}^2 \cdot \text{m}^{-3}$

C_0	Concentration of carbon dioxide in the liquid phases at the inlet of microchannels	$\text{mol}\cdot\text{L}^{-1}$	T'	Temperature of system in the blank experiments	K
C_1	Concentrations of carbon dioxide in the liquid phases at the outlet of microchannels	$\text{mol}\cdot\text{L}^{-1}$	V_{CO_2}	Total CO_2 volume injected into the system in the experiments	m^3
C_2	Concentration of carbon dioxide in the liquid phases in the two-phase collector of experiments	$\text{mol}\cdot\text{L}^{-1}$	V'_{CO_2}	Total CO_2 volume injected into the system in the blank experiments	m^3
C_e	The equilibrium concentration of carbon dioxide in the liquid phases	$\text{mol}\cdot\text{L}^{-1}$	V_{liquid}	Total liquid phase volume injected into the system in the experiments	m^3
C'_2	Concentration of carbon dioxide in liquid phases in the two-phase collector of blank experiments	$\text{mol}\cdot\text{L}^{-1}$	V'_{liquid}	Total liquid phase volume injected into the system in the blank experiments	m^3
D	Liquid phase diffusivity	$\text{m}^2\cdot\text{s}^{-1}$	V	Total volume of the system	m^3
d_h	Hydraulic diameter	m	Greek Letters		
J_G	The gas phase superficial velocity	$\text{m}\cdot\text{s}^{-1}$	σ	Surface tension	N
J_L	The liquid phase superficial velocity	$\text{m}\cdot\text{s}^{-1}$	μ	Viscosity	$\text{Pa}\cdot\text{s}$
k_L	Liquid side mass transfer coefficient	$\text{m}\cdot\text{s}^{-1}$	Dimensionless Group		
$k_L a$	Liquid side volumetric mass transfer coefficient	s^{-1}	Sh_L	Liquid phase Sherwood number	$Sh_L = k_L d_h / D$
L_B	Length of Taylor bubble	m	Sc_L	Liquid phase Schmidt number	$Sc_L = \mu_L / \rho_L D$
L_C	Length of the mixing section of the microchannel	m	Re_G	Gas phase Reynolds number	$Re_G = \rho_G J_G d_h / \mu_G$
L_s	Length of the liquid slug	m	Re_L	Liquid phase Reynolds number	$Re_L = \rho_L J_L d_h / \mu_L$
P_{in}	Inlet pressure of absorption processes	kPa	Ca_L	Liquid phase Capillary number	$Ca_L = \mu_L J_L / \sigma$
P'_{in}	Inlet pressure of absorption processes in the blank experiments	kPa	REFERENCES		
P_{ob}	Outlet pressure before absorption in the experiments	kPa	Bercic, G., Pintar, A., The role of gas bubbles and liquid slug lengths on mass transport in the Taylor flow through capillaries. Chemical Engineering Science, v. 52 (21-22), 3709-3719 (1997).		
P'_{ob}	Outlet pressure before absorption in the blank experiments	kPa	Chisholm, D., A theoretical basis for the Lockhart-Martinelli correlation for two-phase flow. International Journal of Heat and Mass Transfer. v.10, 1767-1778 (1967).		
P_{oa}	Outlet pressure after absorption in the experiments	kPa	Demas, N., Gunther, A., Schmidt, M. A. et al., Microfabricated multiphase reactors for the selective direct fluorination of aromatics. Ind. Eng. Chem. Res. 4, No. 42, 698-710 (2003).		
P'_{oa}	Outlet pressure after absorption in the blank experiments	kPa	Fu T. T., Ma Y. G., Funfschilling D., Li H. Z., Bubble formation and breakup mechanism in a microfluidic flow-focusing device. Chemical Engineering Science, v. 64, 2392-2400 (2009).		
T	Temperature of system in the experiments	K			

- Haverkamp, V., Emig, G., Hessel, V. et al., Characterization of a gas-liquid microreactor. The micro bubble column: determination of specific interracial area. Proceedings of the Fifth International Conference on Microreaction Technology, Berlin (2001).
- Irandoost, S., Andersson, B., Mass-transfer and liquid-phase reactions in a segmented two-phase flow monolithic catalyst reactor. *Chemical Engineering Science*, v. 43, (8), 1983-1988 (1988).
- Irandoost, S., Ertle, S., Andersson, B., Gas-liquid mass-transfer in Taylor flow through a capillary. *Canadian Journal of Chemical Engineering*, v. 70, 115-119 (1992).
- Jähnisch, K., Baerns, M., Hessel, V., et al., Direct fluorination of toluene using elemental fluorine in gas-liquid microreactors. *Fluorine Chem.* 1, No.105, 117-128 (2000).
- Jepsen, J. C., Mass transfer in two-phase flow in horizontal pipelines. *AIChEJ.* 5, No.16, 705-711 (1970).
- Kobayashi, J., Mori, Y., Okamoto, K. et al., A microfluidic device for conducting gas-liquid-solid hydrogenation reactions. *Science*, 304, No. 5675, 1305-1308 (2004).
- Kreutzer, M. T., Hydrodynamics of Taylor flow in capillaries and monolith reactors. Ph.D. Thesis, The Netherlands: Delft University of Technology (2003).
- Liu, G. Q., Ma, L. X., Liu, J., *Manual of Chemistry and Chemical Industry Physicality Data*, Beijing, China, Chemical Industry Press (2002).
- Lockhart R. W., Martinelli R. G., Proposed correlations for isothermal two-phase two-component flow in pipes. *Chemical Engineering Progress*. v. 45, 39-48 (1949).
- Tegrotenhuis, W. E. , Cameron, R. J. , Viswanathan, V. V. et al., Solvent extraction and gas absorption using microchannel contactors. Proceedings of the Third International Conference on Microreaction Technology. Berlin (2000).
- Tortopidis, P. and Bontozoglou, V., Mass transfer in gas-liquid flow in small-diameter tubes. *Chemical Engineering Science*, 14, No.52, 2231-2237 (1997).
- Van Baten, J. M., Krishna, R., CFD simulations of mass transfer from Taylor bubbles rising in circular capillaries. *Chemical Engineering Science*, v. 59, 2535-2545(2004).
- Vandu, C. O., Liu, H., Krishna R., Mass transfer from Taylor bubbles rising in single capillaries. *Chemical Engineering Science*, v. 60, 6430-6437 (2005).
- Yeong, K. K., Gavriilidis, A., Zapf, R., Hessel, V., Experimental studies of nitrobenzene hydrogenation in a microstructured falling film reactor. *Chemical Engineering Science*, 16, No.59, 3491-3494 (2004).
- Yue, J., Chen, G. W., Yuan, Q., Luo L. A., Hervé, L. G., Mass transfer in gas-liquid flow in microchannels. *Journal of Chemical Industry and Engineering*, 6, No.57, 1296-1303 (2006).
- Yue, J., Luo, L. A., Gonthier, Y., Chen, G., Yuan Q., An experimental study of air-water Taylor flow and mass transfer inside square microchannels. *Chemical Engineering Science*, v. 64, 3697-3708 (2009).
- Zhang, S. Q., *Chemical Industry Manual*. Jinan, China, Sandong Science and Technology Press (1986).